Quaternary Geochronology 43 (2018) 83–90

Contents lists available at ScienceDirect

Quaternary Geochronology

journal homepage: www.elsevier.com/locate/quageo

Research paper

Building robust age models for speleothems – A case-study using coeval twin stalagmites

Alexa Benson[a,*], Dirk L. Hoffmann[a], Pavel Bella[b,c], Anna Joy Drury[d,e], Helena Hercman[f], Timothy C. Atkinson[d]

[a] Max Planck Institute for Evolutionary Anthropology, Department of Human Evolution, Deutscher Platz 6, 04103 Leipzig, Germany
[b] State Nature Conservancy of the Slovak Republic, Slovak Caves Administration, Hodžova 11, 031 01 Liptovský Mikuláš, Slovakia
[c] Catholic University in Ružomberok, Pedagogical Faculty, Department of Geography, Hrabovská Cesta 1, 034 01 Ružomberok, Slovakia
[d] Department of Earth Sciences, University College London, WC1E 6BT, UK
[e] MARUM, University of Bremen, Bremen 28359, Germany
[f] Institute of Geological Sciences, Polish Academy of Sciences, Twarda 51/55 St., 00-818 Warszawa, Poland

ARTICLE INFO

Keywords:
U-series
Coeval stalagmites
Twin stalagmites
Palaeoclimate
Stable isotopes
Trace elements
Holocene
Central Europe
Slovakia
Western Carpathians
Chronology

ABSTRACT

We use the uranium-series (U-Th) dating method to investigate the accuracy of a relative chronology based on laminae correlation between a pair of coeval twin stalagmites and compare their stable isotope and trace element records based on the two chronologies. U-Th dating shows that a relative chronology based on laminae correlation can be inaccurate: a hiatus in one of the stalagmites was not recognised, as well as more subtle changes in growth rates. Use of the stratigraphic correlation alone resulted in significant differences in the timing of stable isotopes and trace element peaks, with implications for their interpretation. Our results reveal the importance of a robust and direct chronology with which to interpret proxy data. Poor relative chronologies can lead to a misinterpretation of palaeoclimate data. The study reveals potential implications for speleothem records where proxy data and samples for dating were not taken in close proximity to each other and/or were correlated via laminae over distances of more than a few centimetres.

1. Introduction

Karstic systems are home to a host of (geochemical) archives, which can be used to reconstruct local and regional palaeoenvironmental and climatic conditions. Speleothems, such as stalagmites and flowstones, provide multiple palaeoclimatic and environmental proxies, with chronological constraints provided principally by U-Th dating (see e.g. Fairchild and Baker (2012) for a recent overview). Here we describe a case study in chronology-building that exploits the replication provided by twin stalagmites deposited only a few centimetres apart and joined by coeval flowstone. Modern analytical and measurement techniques permit the selection of very small samples for U-Th dating (Hoffmann et al., 2007; Hoffmann, 2008), allowing closely-spaced sampling along the growth axis of a stalagmite and the building of very detailed chronologies and age models (Scholz et al., 2012). In the past decades, many dated records of geochemical proxies for palaeoclimate and environment have been published (Fairchild and Baker, 2012). Most have relied on single stalagmite or flowstone specimens, while others are based on composite records by correlation between specimens with overlapping periods of deposition (Fohlmeister et al., 2012, 2013; Bar-Matthews et al., 1998; Bar-Matthews and Ayalon, 2011; Kelly et al., 2006; Spötl et al., 2006; Yuan et al., 2004; Wang et al., 2001). Though composite records rely on multiple, partially coeval specimens, each one is usually isolated from all other specimens in the record, whether located in the same cave (e.g. Soreq, Spannagel) or in caves that are some distance apart (e.g. China: Hulu/Dongge, Israel: Soreq/Peqiin (Bar-Matthews et al., 2003)). Such correlation of proxy records between specimens is made in the time domain and therefore relies upon the robustness and accuracy of the age models for individual specimens (Spötl et al., 2006). Historically, age models have developed from the extremely simple, e.g. interpolation between just two dates located near the top and bottom of the specimen, to very detailed and robust, with dates at multiple levels providing constraints on varying growth rates within the specimen, identifying gaps in growth (hiatus), and defining the overall time period represented. Recently published records may be supported by chronologies with several tens of dates in sequence on a

* Corresponding author.
E-mail addresses: alexa_benson@eva.mpg.de (A. Benson), dirk.hoffmann@eva.mpg.de (D.L. Hoffmann), pavel.bella@ssj.sk (P. Bella), ajdrury@marum.de (A.J. Drury), hhercman@twarda.pan.pl (H. Hercman), t.atkinson@ucl.ac.uk (T.C. Atkinson).

http://dx.doi.org/10.1016/j.quageo.2017.10.004
Received 11 May 2017; Received in revised form 10 October 2017; Accepted 24 October 2017
Available online 31 October 2017
1871-1014/ © 2017 The Authors. Published by Elsevier B.V. This is an open access article under the CC BY license (http://creativecommons.org/licenses/BY/4.0/).

single stalagmite, giving a high degree of confidence in the chronology and allowing age uncertainties to be calculated for every position along the axis of the specimen. While scientifically desirable, such a thorough approach requires relatively unrestricted access to modern dating facilities, which is not always available. This lack in funds or facility access may compromise the reliability of correlations made in the time domain, for example when attempting to make spatial maps of proxies for specific time horizons (McDermott et al., 2011). Within a single specimen, it is common practice to locate drilled or micro-milled samples and/or *in situ* analyses of the various geochemical proxies along different tracks, and then to rely upon visible layering or lamination to establish correlations between them.

In this study, we recount our experience in dating and stratigraphic correlation between twin stalagmites joined at their bases by visibly-laminated flowstone calcite that was precipitated from the same drip waters. Stratigraphic correlations were made between the twin specimens based on (a) visible layering, (b) proxy geochemical records made along their growth axes, and (c) independent age models using a total of 27 U-Th ages. In this paper, we focus on the chronology that is needed to compare proxy data between twin stalagmites, and consider the implications for the general methodology of speleothem inter-comparison and correlation.

1.1. Study site and samples

The Demänovská jaskyňa slobody Cave (Demänovská Cave of Liberty) (48°59′N, 19°34′E) is located on the northern side of the Nízke Tatry (Low Tatra) Mountains, Northern Slovakia, situated beneath the eastern slope of the Demänovská Valley (Motyka et al., 2005). This cave is a part of the extensive multi-levelled Demänová cave system formed by sinking allochthonous streams passing through the Middle Triassic Gutenstein limestones of the Krížna Nappe (McCann, 2008). The cave system is generally oriented in a north-south direction, along the eastern side of the Demänovská Valley (Bella et al., 2014; Droppa, 1957, 1966a, 1966b, 1972). It is 41 km long and is the largest and longest known karst system in Slovakia (Herich, 2015). The vertical span between the lowest and highest places of the cave system is 196 m, at an elevation of 772–968 m above sea level. The bedrock thickness above the various parts of the cave ranges from 40 to 270 m (Motyka et al., 2005).

A pair of twin stalagmites (HcH2A and HcH2B) was collected in the cave in September 2004. The specimen represented a clear opportunity to study the degree to which geochemical proxies are replicated in different specimens formed in very close proximity. The site of their deposition was a small chamber in a western side-passage of the Hlinená chodba. At the time of collection, the stalagmites had been moved from their original location because of excavation efforts made by cave explorers hoping to extend a mud-filled passage beyond the chamber. There were several drip points from the chamber roof, including two that were a similar distance apart as the stalagmites. One of these drip points was the tip of a small stalactite, the other a fracture. They were suspected to be the parent drip sources. Several of the factors that influence speleothem proxy compositions, such as cave temperature, ventilation, humidity and CO_2 content of the air would all have been identical for the coeval layers of the two stalagmites. Other factors such as drip rates, chemistry and exact isotopic compositions of the two drips may not have been identical, although it seems unlikely that $\delta^{18}O$ differed greatly between drip locations only 10–12 cm apart. Three drip samples collected from the chamber on 5–6 September 2004 had a range in $\delta^{18}O$ of 0.5‰ and mean of −9.7‰. This overlaps the weighted mean of −9.8‰ for the previous 12 months of precipitation at the nearby GNIP station at Liptovsky Mikulas-Ondrasova (alt. 570 m), suggesting that mixing in the bedrock above the cave may homogenise the seasonal cycle of $\delta^{18}O$ in precipitation to some extent. The long-term weighted mean for precipitation in calendar years 1992–2015 is −9.70‰ with standard deviation 1.13‰ (Holko et al., 2012; IAEA/WMO, 2017).

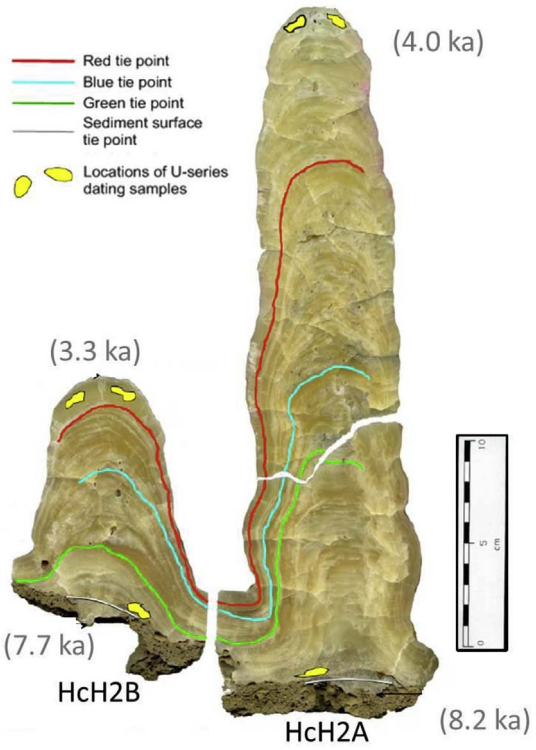

Fig. 1. Stratigraphic correlation tie point locations, shown in green, blue and red. Sample positions for preliminary U-Th dates are in yellow. Bracketed values are provisional dates calculated in 2005, which suggested a likely Holocene age and possibly coeval growth for both stalagmites. They are not used further in this paper. (For interpretation of the references to colour in this figure legend, the reader is referred to the web version of this article.)

1.2. Initial analyses

Soon after collection, preliminary U-Th dates (Fig. 1) were obtained for samples taken near the top and bottom of each stalagmite, placing the time of formation of the two specimens between 10 ka and 3 ka. The geochemical records of the stalagmites were also initially analysed, first for $\delta^{18}O$ and $\delta^{13}C$ (2006/2007) and later for Mg/Ca and Sr/Ca (2010). However, no additional dating was possible until 2015/2016.

In 2008, the layering and laminae that were visible in the segment of flowstone joining the stalagmites were examined in detail. It was not straightforward to trace the laminae unambiguously up the sides of the stalagmites and thus join them to the laminae and layering visible at the summit of each specimen. Nevertheless, it was thought at the time that the stratigraphic correlations shown in Fig. 1 were at least approximately correct and might allow a correlation to be made between the proxy records obtained from the axial parts of each stalagmite (Atkinson et al., 2008). The relative chronology and subsequent interpretation were put to the test when the two stalagmites were carefully dated in 2015/2016.

2. Material and methods

HcH2A measures 334 mm in length, while the shorter twin stalagmite, HcH2B, measures 120 mm. The whole specimen, i.e. both stalagmites, was cut along the plane containing both growth axes using a diamond-coated circular saw, producing approximately 1.5 cm thick slabs as shown in Figs. 1 and 3. The surfaces were then polished to reveal crystal structure and colour laminations, which vary from translucent white to light cream and pale brown in colour. No definitive growth hiatuses were observed along the growth axes of either

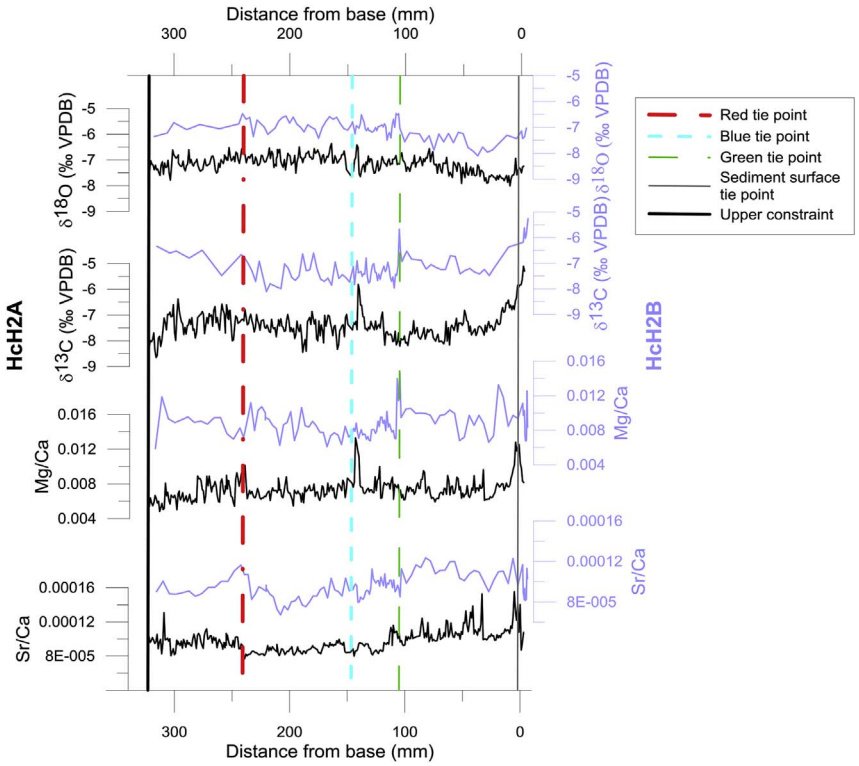

Fig. 2. Stable isotope and trace element values for HcH2A and HcH2B graphed against the interpolated linear distance (mm) from an arbitrary datum level on HcH2A. The data from the shorter stalagmite, HcH2B, was transposed onto the distance scale of the longer HcH2A by linear interpolation between five tie points. These tie points are illustrated in Fig. 1 and shown here as vertical lines: the coloured lines indicate the stratigraphic correlation tie points, while the grey indicates the sediment surface location. The calcite in both stalagmites is assumed to be contemporaneous at the tie points. (For interpretation of the references to colour in this figure legend, the reader is referred to the web version of this article.)

stalagmite.

Sub-samples for U-Th dating, stable isotope analyses and trace element analyses were collected using a hand-held micro drill. U-Th samples for MC-ICPMS analyses with masses ranging between 19 and 40 mg were collected from isolated layers along the growth axis for both stalagmites. Stable isotope sampling for analysis was done at 1 mm intervals from the base to top of HcH2A and HcH2B. Trace element sampling for ICP-AES analyses was also done at 1 mm intervals from base to top of HcH2A and HcH2B, with special care taken to ensure that the location of both trace element and stable isotope data corresponded accordingly.

2.1. Stratigraphic correlation

Scanned images were made of the slabs at a resolution of 600 dpi. These were studied while enlarged approximately three-fold on a computer screen, i.e. image pixels were ca. 200 dpi. Microscopic textural changes such as those systematically described by Frisia (2015)

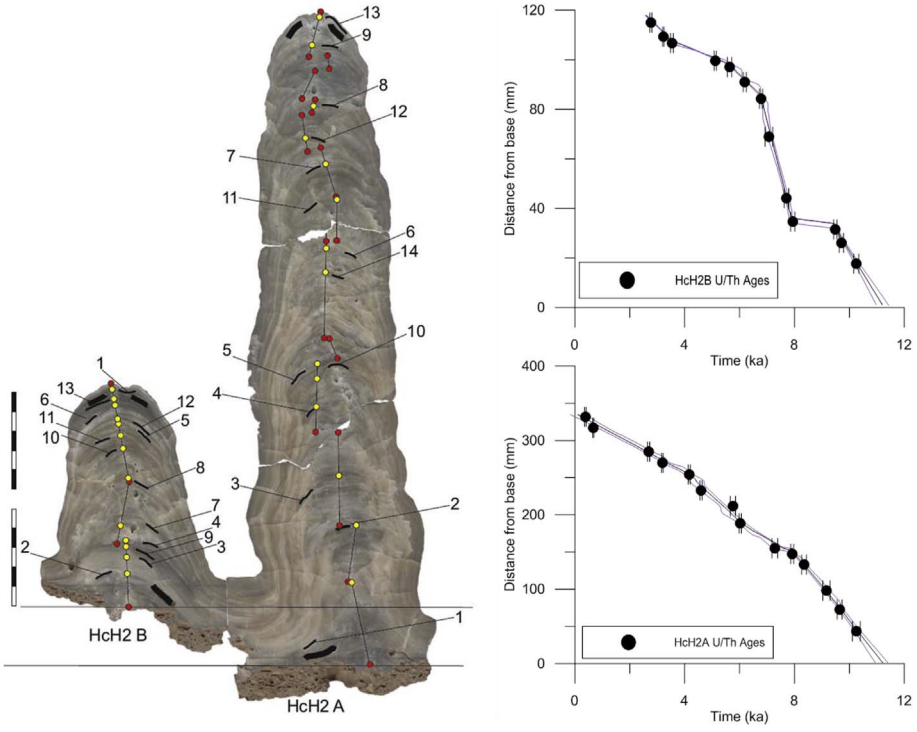

Fig. 3. Left: HcH2A and HcH2B speleothem slabs with sample locations (right). The preliminary dates are shown as thick black lines (cf. Fig. 1), located at the upper-most and lower-most portion of each specimen. The sample locations for the U-Th dates measured in 2015–16 are shown in black and indicated with sample number, the yellow dots locating the sampling location with respect to the central growth axis. The arrowed numbers indicate the identifier of each date as listed in Table 2 (Supplemental Materials) where the numbers are prefixed by the code for the stalagmite, e.g. HcH2B#1. The sampling tracks for stable isotopes and trace elements are indicated by black lines with a red dot at both ends of each section of track.
Right: Age models for HcH2A (bottom) and HcH2B (top) created using the algorithm StalAge (Scholz and Hoffmann, 2011). The dates are shown with 2σ error bars. The central black line represents the mean age, with outlying lines indicating the 2σ uncertainty bands. (For interpretation of the references to colour in this figure legend, the reader is referred to the web version of this article.)

could not be distinguished at this low level of magnification. Visible laminae and growth surfaces were identified primarily on the basis of contrasts in colour. Some laminae and growth surfaces that were clear in one place changed in colour when followed laterally and no longer contrasted sufficiently with the calcite above or below them. Nevertheless some features were persistent and lateral tracing of these was begun in the central section joining the two stalagmites. Two growth horizons, shown as red and green lines on Fig. 1 could be traced unambiguously through this section. The third (blue) was more difficult to follow from the lowest part of the flank of HcH2A, where it was well defined, because of thinning and inter-fingering of layers at the lower flank of HcH2B. Tracing laminae from the central flowstone section up the sides of the stalagmites was also difficult in the near-vertical sides of HcH2A where they were very thin and crowded together. With hindsight it seems likely that this is where significant errors were made, either because the layers were so thin that they could not be traced accurately or because colour features may have been diachronous (i.e. the visible feature may have appeared to be continuous but its age actually varied along its length). Once the red, green and blue laminae had been defined and traced to the tops of the stalagmites, correlation between the two records was made by linear interpolation and rescaling of the axial profile of HcH2B onto the longer axial scale of HcH2A. It was assumed that both stalagmites commenced and finished growth at the same time. The surface of the muddy sediment beneath each had been penetrated by a shallow pit formed by the dripping water that eventually deposited the stalagmites (Fig. 1). Distance scales were defined following the growth axes. The zero points for these scales were lines defined at arbitrary levels a little distance above the base of each stalagmite. The axial distances of all the tie points relative to these arbitrary datum levels are listed in Table 1 of the Supplemental Materials. By means of linear interpolation between the 'tie-points', proxy data could be transferred from the distance scale of the shorter HcH2B stalagmite onto the scale of HcH2A, as shown in Fig. 2.

2.2. U-Th chronology

Initial U-Th dates were obtained in 2005 shortly after collection. Samples of about 500 mg were processed at the University of East Anglia and measured using a newly-acquired MC-ICPMS Nu instrument at the University of Cambridge at a stage when spike solutions and potential fractionation effects during measurement had not been fully calibrated. Sample measurements of U and Th were alternated with standard solutions to determine mass-dependent fractionations during ionisation of each element. Unfortunately no Th standard was available with a low ^{232}Th concentration designed to match secondary carbonates. One designed for igneous rocks was used instead, with a much higher concentration of ^{232}Th than the sample solutions. This difference may have affected the corrections obtained for mass-dependent fractionation during ionisation. Additional uncertainty regarding the calibration of the ^{229}Th spike solution may account for the discrepancies between the preliminary dates calculated in 2005 and the much more rigorous measurements made in our 2015/16 study. The preliminary work was curtailed by the abrupt departure of one of the project personnel and there was no subsequent opportunity to make better calibrated measurements. Notwithstanding these issues, the provisional results calculated in 2005 suggested that both stalagmites probably formed during the Holocene. Fig. 1 shows the purely nominal ages obtained from this incomplete preliminary work. These values are not used in the remainder of this paper.

For the present study, undertaken in 2015/2016, U-Th dating of the two stalagmites was done on a total of 14 samples for HcH2A and 13 samples for HcH2B. The samples were processed and analysed at the Max Planck Institute for Evolutionary Anthropology (MPI-EVA) in Leipzig, Germany. A, double resin procedure was used for chemical separation and purification of U and Th for MC-ICPMS, as described by Hoffmann et al. (2016). Uranium-series measurements were undertaken on a ThermoFinnigan Neptune MC-ICPMS with a Cetac Aridus II and a Savillex PFA 50 µl/min microconcentric nebulizer. Refer to Hoffmann et al. (2007) for further details regarding measurement methods, including standards and protocols used to assess and correct instrumental biases. An age model for each stalagmite was created using StalAge (Scholz and Hoffmann, 2011).

2.3. Stable isotope analyses

Stable isotope records for δ^{18}O and δ^{13}C were processed at the Bloomsbury Environmental Isotope Facility (BEIF), University College London. In total, 333 sub-samples were drilled along the growth axis of HcH2A and 121 were drilled for HcH2B. Samples were measured using a Thermo Delta Plus mass spectrometer with a Gasbench II preparation system. Precision determined from 34 analyses of standard NBS19 in separate runs was ± 0.06‰ (1-standard deviation) for both δ^{18}O and δ^{13}C.

2.4. Trace element analyses

333 separate sub-samples were drilled along the growth axis of HcH2A and 121 were drilled for HcH2B, alongside the holes previously drilled for stable isotope analysis. All samples were acidified in 3 ml 5% HCl one day before analysis to ensure complete dissolution. Blanks were prepared simultaneously to ensure no trace elements were added by leaching from the sampling tubes. Samples were analysed for Ca, Mg, and Sr by atomic emission spectroscopy using a *Jobin-Yvon Ultima 2C ICP-AES*. Prepared aliquots of standard solutions were used to calibrate concentrations and correct for instrument drift. Analytical uncertainties (1 standard deviation) were approximately 2% of average values in the stalagmites for Sr/Ca and 3% for Mg/Ca.

3. Results and discussion

3.1. Comparison of geochemical records within the relative chronology

Before the U-Th ages were available along both growth axes, the two speleothems were stratigraphically correlated as described above. This correlation provided a relative chronology within which the stable isotope records obtained from the two stalagmites could be compared (Atkinson et al., 2008). Fig. 2 shows this comparison to emphasise the similarities and differences in the long period trends.

The records for δ^{18}O display some agreement, with similar long-term trends, similar ranges of values (−8.0 to −6.36‰ for HcH2A, −8.1 to −6.47 for HcH2B) and nearly identical average values (−7.15‰ for HcH2A and −7.17‰ for HcH2B). Although there is considerable discrepancy in second order variability (Fig. 2), it was thought that this could be partly explained by the different temporal sampling frequencies. Overall, the good first order agreement for δ^{18}O appeared to support the validity of the stratigraphic correlations between the two stalagmites.

Notably, the addition of trace element data a few years later did not seem to undermine the stratigraphic correlation. Fig. 2 shows that the Sr/Ca records have an agreement in long-term trends that is only slightly less than that for δ^{18}O. Average ratios (w/w) are similar, 9.72×10^{-5} for HcH2A and 9.58×10^{-5} for HcH2B. The discrepancy in short-term features appears much larger between the Sr/Ca records than for δ^{18}O. At the time this was attributed to differences in sampling frequency, although this is unlikely to explain the larger range of values displayed by HcH2B between about 200 and 250 mm on the distance scale in Fig. 2.

The δ^{13}C and Mg/Ca records in Fig. 2 do not show the same good long-term trend replication between the stalagmites as seen in δ^{18}O and Sr/Ca. For δ^{13}C there is some similarity in long-term trends but the values for the smaller stalagmite HcH2B tend to be higher. Both records display a sharp spike in δ^{13}C but these occur at different positions on

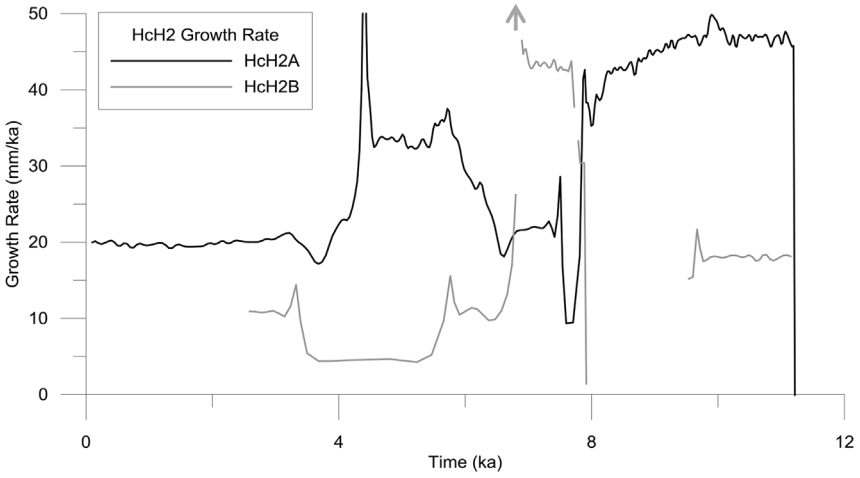

Fig. 4. Linear extension rates for HcH2A (black line) and HcH2B (grey line), plotted against time (ka). The data have been calculated using model age estimates every mm along the stalagmites' axes. This introduces short-term variations in growth rate that are largely artefacts of the StalAge algorithm. To smooth these, the broken lines show moving average values for each stalagmite, calculated with spans equal to the time intervals between successive dates.

the stratigraphically correlated distance scale, at ca. 140 mm in HcH2A and at a correlated distance of 106 mm for HcH2B (Fig. 2). For Mg/Ca the discrepancies are greater. There is good agreement in values for a short section between ca. 110 and 165 mm but elsewhere the values for HcH2B are consistently higher than for the longer HcH2A stalagmite, with 19% higher average values (8.76×10^{-3} for HcH2B vs 7.37×10^{-3} for HcH2A). The highest spikes in each record occur at the same offset positions as the spikes already noted for $\delta^{13}C$. Though the Mg/Ca records for both stalagmites are more variable and 'spiky' than Sr/Ca, the agreement between the temporal positions of the spikes is poor.

At this stage, the interpretation of the geochemical data was based on the acceptance of the relative chronology, supported by the good agreements in first-order trends for $\delta^{18}O$ and Sr/Ca. Discrepancies in second-order features were interpreted as mainly due to differences in temporal sampling frequency caused by the different heights of the two stalagmites. The much greater differences between them for $\delta^{13}C$ and Mg/Ca were interpreted as due to factors that were specific to each stalagmite. It was thought the higher $\delta^{13}C$ values in HcH2B might reflect a slower drip rate and longer CO_2 degassing times, a notion that was in accord with its smaller size and apparently slower rate of growth.

The data for Mg/Ca and Sr/Ca seemed to fit with this interpretation. Sr/Ca showed an overall good agreement between the two records, whereas for Mg/Ca there were important differences, with the average value for HcH2B about 19% higher than for HcH2A. As the chemistry of the source water reaching the cave roof was likely the same for both, the differences were attributed to a difference in the amount of prior calcite precipitation (PCP). Thus, HcH2A was envisaged as forming more quickly than its neighbour because of a faster drip rate, while HcH2B may have grown more slowly because of slower drip rate and PCP of a possible stalactite above it.

Atkinson et al. (2008) gave the comparison of $\delta^{18}O$ in these stalagmites as an example of natural replication of stable isotope records, an inference that required the prior assumption that the stratigraphic correlations were valid and demonstrated contemporaneity. The addition of trace element data gave modest confidence that the two stalagmites demonstrated good replication of $\delta^{18}O$, reflecting their common water source, and Sr/Ca reflecting a commonality in the transit time of water from the cave roof, as well as any external sources of Sr (Fairchild et al., 2006; Baldini et al., 2006; Borsato et al., 2007; Fairchild and Hartland, 2010). The difference between the $\delta^{13}C$ and Mg/Ca of the twin speleothems could be explained in terms of factors affecting each speleothem individually, namely differences in drip rates and PCP. This interpretation fitted well into prevailing paradigms in speleothem palaeoclimatology (Fairchild and Baker, 2012) but it was based on a false premise, as subsequent U-Th dating revealed.

3.2. Comparison of geochemical records within the U-Th based chronology

In 2015/2016, independent and robust U-series chronologies were generated for the two stalagmites. U-series results and age models for HcH2A and the twin sample HcH2B are illustrated in Fig. 3 and additional details can be found in Table 2 of the Supplemental Materials.

Samples for U-Th analysis were taken from the most pristine layers, avoiding sections with any visible dirt inclusions (Fig. 3). The ^{232}Th concentrations, indicative for detrital contamination, are generally < 1 ng/g, and only two samples have values between 1.5 and 2 ng/g. The $^{230}Th/^{232}Th$ activity ratios are generally > 100.

For both specimens, the calculated dates are in strict stratigraphic order. Fig. 3 shows independent distance-age models based on all the 2015/16 U-Th dates for each stalagmite with interpolated values and associated confidence levels generated using the StalAge algorithm (Scholz and Hoffmann, 2011). For HcH2A, we find continuous growth through the Holocene (10.31 ± 0.14 ka to 0.49 ± 0.02 ka), with no observable growth-stops. The overall average growth rate is 34.6 mm/ka. Fig. 4 shows the record of growth rate derived from the StalAge model. Three 'stepped decreases' in growth speed are observed towards the present. Initial growth is fastest between 11 ka and 8.44 ka (~44 mm/ka), followed by a notable trough at ~7.9 ka, where rates decrease to 10 mm/ka (Fig. 4). Between 7.8 ka and 6.2 ka, the growth rate is around 22 mm/ka, followed by a surge to a plateau between 5.8 and 4.3 ka that averages about 34 mm/ka. From 4.3 ka growth rate drops, averaging 19.3 mm/ka towards the present.

HcH2B largely formed between 10.25 ± 0.09 and 2.8 ± 0.04 ka, but here the stalagmite growth is more episodic (Fig. 3). The StalAge algorithm identifies one growth-stop, between 9.49 ± 0.64 and 7.94 ± 0.08 ka. Between 11.2 and 9.4 ka, growth rate averages 18 mm/ka (Fig. 4). In contrast to HcH2A, the smaller stalagmite reached its fastest growth rate of 44 mm/ka between 7.75 and 6.8 ka, directly following the hiatus. After 6.8 ka, growth rate decreases considerably, averaging 9.89 mm/ka in the last growth episode which stopped around 2.8 ka. During periods when it was being actively deposited, the overall average growth rate for HcH2B of was 30.54 mm/ka, which is only slightly smaller than for HcH2A.

Uranium concentrations are relatively constant and similar for both stalagmites with values ranging between 271 ng/g and 168 ng/g (Fig. 5). Mean values for A and B are almost identical at 212 ng/g. The U concentrations initially increase for both stalagmites from values around 210 ng/g to 'peak' concentrations around 270 ng/g at 9.25 ka, then slightly decrease again and fluctuate around a mean value of about 180 ng/g before rising again to values around 200–210 ng/g (Fig. 5). The youngest sample in HcH2A shows a decrease to ca. 170 ng/g. The concordance of concentration values and synchronous evolution indicates a shared water source for the two stalagmites and no significant

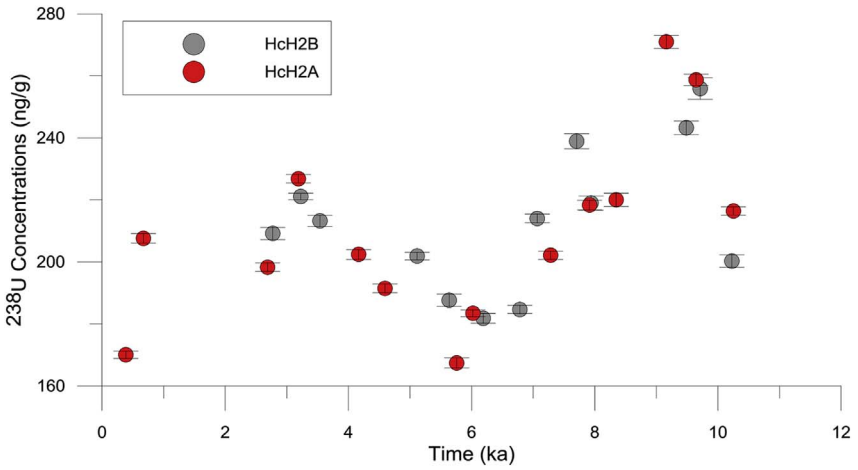

Fig. 5. ^{238}U concentrations for coeval stalagmites HcH2B (grey) and HcH2A (red) are plotted against age. Error bars signify 2σ uncertainty. (For interpretation of the references to colour in this figure legend, the reader is referred to the web version of this article.)

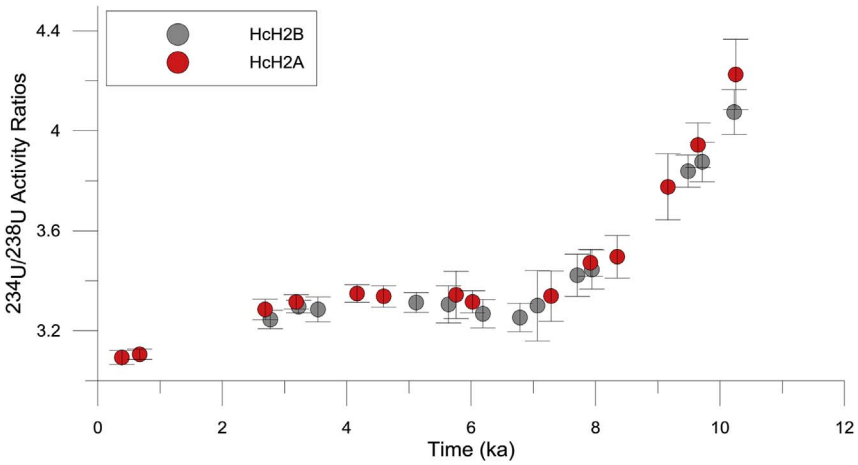

Fig. 6. Initial $^{234}U/^{238}U$ activity ratios for coeval stalagmites HcH2B (grey) and HcH2A (red) are plotted against age. Error bars signify a 2σ uncertainty. (For interpretation of the references to colour in this figure legend, the reader is referred to the web version of this article.)

effect of growth rate on U concentrations.

The initial $^{234}U/^{238}U$ activity ratios calculated for the two stalagmites display a strong coherence (Fig. 6). Initial $^{234}U/^{238}U$ activity ratios were highly elevated with values around 4.2 when the stalagmites started forming. The ratios then steadily decreased reaching values around 3.3 by 7 ka, which is still highly elevated when compared with many secondary carbonates (Latham and Schwarcz, 1992) and oxic ground waters in carbonate aquifers (Osmond and Cowart, 1992; Osmond and Ivanovich, 1992). The initial $^{234}U/^{238}U$ activity ratio forms a plateau with values around 3.3 between 7 ka and 2.5 ka when HcH2B stopped forming. The younger top samples of HcH2A show slightly lower values of ~3.1. The $^{234}U/^{238}U$ activity ratios of the two stalagmites have the same absolute values and show the same temporal evolution, again suggesting that the water source is shared and that neither U concentrations nor growth rate seem to correlate with $^{234}U/^{238}U$. For further detail regarding chemistry results and calculations for both specimens, please refer to Table 2 in the Supplemental materials.

3.3. Comparison of relative and U-Th chronologies

When comparing the two chronological methods, the most notable outcome is how significantly the synchronicity between stalagmites differs between methods. The U-Th dating revealed fundamental shortcomings in the stratigraphic correlation technique. Levels in the stalagmites' axial regions that layer tracing had suggested were contemporaneous were revealed to differ in age by offsets of 0.99 ka (green line on Fig. 1), 0.77 ka (blue line) and 0.47 ka (red line). All three lines were first identified in the flowstone between the stalagmites and then traced upwards into the stalagmites themselves, first into HcH2B then into HcH2A. The tracing of the green line into HcH2A placed it too low to be time-equivalent to its partner in HcH2B. According to the age models it should have been placed in approximately the position of the blue line and the latter should have been placed about 17 mm higher. Although the stratigraphic laminae correlation attempted to address issues such as disparity in laminae thickness and growth rate, it ultimately failed because the colour changes that defined the layering in HcH2A were difficult to follow unambiguously. The two stalagmites did not cease growth at the same time, as HcH2A continued to be deposited for 2.5 ka after growth of HcH2B had stopped. However the assumption that the commencement of growth took place at the same time for both was confirmed by the U-Th dating, as the extrapolated ages for the bases of both are indistinguishable within error (Fig. 3).

3.4. Replication of geochemical records in the U-Th chronological framework

Using the U-Th derived chronologies, stable isotope values and trace element ratios were re-plotted against time for both HcH2A and HcH2B (Fig. 7). The highest resolution is in HcH2B between 8 and 6.5 ka (Fig. 7b), while after this the resolution for HcHB2 is much smaller than for HcH2A. In the period of overlap between 11 and 9.5 ka, the resolution is comparable for both. The most striking change from Fig. 2 is that in the U-Th age models the two most significant peaks for $\delta^{13}C$ and Mg/Ca are synchronous within uncertainties at 7.9 ka. Additionally, both records share a similar decrease in $\delta^{13}C$ values between 11.2 ka and 9.49 ka, and both records have a synchronous peak around 10.3 ka for Mg/Ca (Fig. 7). Overall, based on the direct U-Th chronology, we

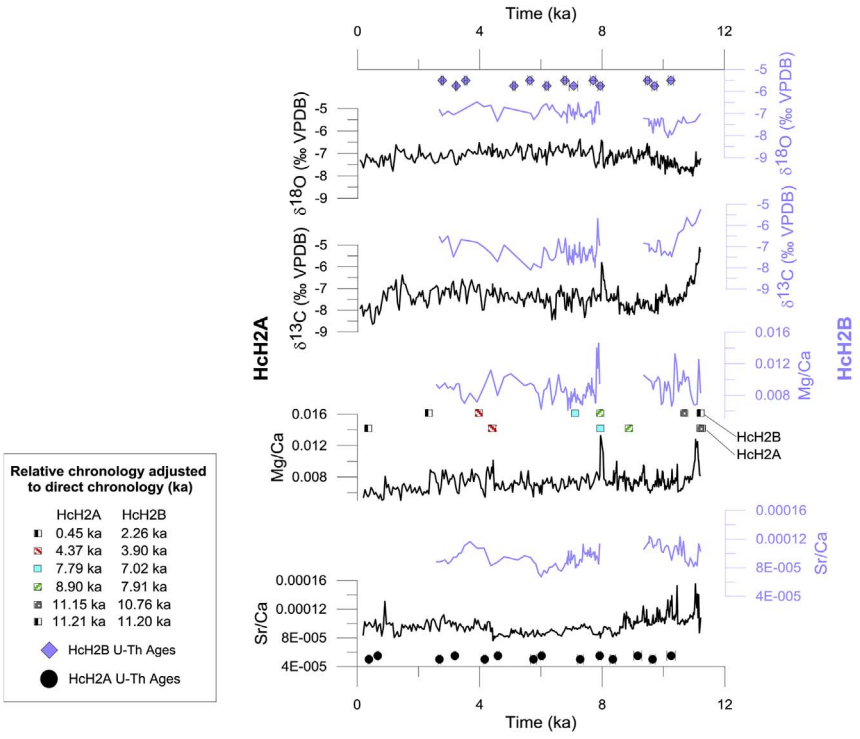

Fig. 7. a. Stable isotope and trace element values for both HcH2A (left, black line) and HcH2B (right, purple line) graphed against time (in ka), using our direct U-Th chronology. U-Th dates (purple diamonds for HcH2B above and black circles for HcH2A - below) are shown with 2σ error. The coloured squares overlying the data correspond to the stratigraphic correlation tie points located on the stalagmite profiles (Figs. 1 and 2). The black-and-white squares refer to the first and last calcite deposition of the stalagmites, while the grey indicates the sediment surface location. The stratigraphic correlation tie points for HcH2B are positioned above, while the boxes for HcH2A are positioned below their respective plots. These boxes help illustrate the extent to which the stratigraphic tie points were incorrectly positioned. (For interpretation of the references to colour in this figure legend, the reader is referred to the web version of this article.)

find an improved coherence of the $\delta^{13}C$ and Mg/Ca records for the two stalagmites between 11 and 6 ka. The low resolution of the younger section of HcH2B however does not allow a detailed comparison. For $\delta^{18}O$ and Sr/Ca the coherence is also good for the major period of overlap, but less so in the period before 9.5 ka. The Sr/Ca ratios appear to be negatively correlated between 11.2 and 9.5 ka.

3.5. Implications for speleothem palaeoclimatology

We have described two methods employed for palaeoclimate reconstruction. While we acknowledge that the original relative chronology based on stratigraphic correlation provides uncertainties that the data alone cannot help distinguish, the comparison of the two methods and interpretation of results has useful methodological implications. Most notably, the relative chronology does not allow for comparison to other proxy records in a common reference time-frame. Without an absolute/independent chronology, one simply cannot compare the proxy records to other regional records in order to understand their spatial context. However the twin stalagmites provide an opportunity to compare records that should be very similar to each other because the specimens themselves formed under near-identical conditions. The accuracy and precision of the independent U-Th age models for the specimens can be tested by examining whether the proxy records show coherent replication within predicted uncertainties. Single speleothems do not normally provide such an opportunity. Because the relative chronology preceded all the high-precision U-Th dating, our study also provides an objective test of the value and pitfalls in making stratigraphic correlations using the visible layering in speleothems. Ultimately, the previous failure to make accurate stratigraphic correlations emphasises that speleothem laminations are difficult to follow visually and use to assign coeval sections. In many cases a variety of proxies and chronologies are measured on different sections of a speleothem which need to be projected or translated onto a shared distance axis. Our study shows potential problems associated with projecting proxy data and chronology onto one central axis, especially where correlation of proxy data records is done over long distance, e.g. for large flowstone sections or through the thin laminae in the sides of stalagmites. Our results demonstrate that correlation can fail where laminae are followed over distances of more than a few centimetres and that sub-sampling for proxy data and dating needs careful planning and should be as close as possible. Similarly, on a larger scale one must be cautious where flowstone dating results from one part of a cave are used to infer ages of distant sections of the apparently continuous flowstone layers (Liu et al., 2015). Use of lamina control points for relative chronologies does not allow for the identification of growth hiatuses even if these control points are correctly associated, because this method must assume that points that are proportionally spaced between tie points in both stalagmites are synchronous. Our U-series chronology is substantiated with 27 U-Th dates, with no reverse dates or indication of open-system behaviour. The incorporation of our independent chronology significantly increases the degree of coherence between the two records not previously observed by the laminae correlation.

4. Conclusion

The principal lesson to be drawn from the erroneous interpretations we made after preliminary stratigraphic correlation is that even a study on coeval stalagmites to assess local cave effects needs a robust independent chronology. Without that, no comparison can be made to reliably identify local cave environmental influences. Given the complicated structure of speleothem lamination, it is not acceptable simply to correlate such materials stratigraphically. Our study highlights the importance of a direct chronology in any wider palaeoenvironmental study. However, we acknowledge that not all research facilities are in a position to process and obtain a similar high density of U-series dates for speleothem chronologies.

From our experience with this twin specimen we conclude that,

(1) Speleothem laminae may be partially diachronous and more complex than visual inspection might suggest.
(2) Even a careful correlation of laminae produces unreliable correlations over distances of more than a few centimetres.
(3) An adequate, independently-dated chronology for stable isotope and trace element records is essential for inter-record comparisons and palaeoclimate reconstruction.

Acknowledgements

We thank the UK Natural Environment Research Council for support (NERC **NER/T/S/2002/00460**, *IsomapUK: A combined data-modelling investigation of water isotopes and their interpretation during rapid climate-change events*), Peter Rowe, Paul Tilyard, Claire Ricketts and Tony Osborne for laboratory assistance, and Tomas Nowicki, Ditta Kicińska and Sarah White for help in the field. We thank two anonymous referees and the journal Editor for comments that significantly improved this paper.

Appendix A. Supplementary data

Supplementary data related to this article can be found at http://dx.doi.org/10.1016/j.quageo.2017.10.004.

References

Atkinson, T., Osborne, A.H., White, S., et al., 2008. Unison, harmony or cacophony? Similarities and differences among coeval isotope records from near-neighbour speleothems. Geophys. Res. Abstr. 10. http://www.cosis.net/abstracts/EGU2008/10244/EGU2008-A-10244.pdf.

Baldini, J.U.L., McDermott, F., Fairchild, I.J., 2006. Spatial variability in cave drip water hydrochemistry: implications for stalagmite paleoclimate records. Chem. Geol. 235, 390–404.

Bar-Matthews, M., Ayalon, A., 2011. Mid-Holocene climate variations revealed by high-resolution speleothem records from Soreq Cave, Israel and their correlation with cultural changes. Holocene 21, 163–171.

Bar-Matthews, M., Ayalon, A., Gilmour, M., et al., 2003. Sea–land oxygen isotopic relationships from planktonic foraminifera and speleothems in the Eastern Mediterranean region and their implication for paleorainfall during interglacial intervals. Geochim. Cosmochim. Acta 67, 3181–3199.

Bar-Matthews, M., Ayalon, A., Kaufman, A., 1998. Middle to Late Holocene (6,500 yr. period) paleoclimate in the Eastern Mediterranean region from stable isotopic composition of speleothems from Soreq Cave, Israel. In: Water, Environment and Society in Times of Climatic Change. Springer, pp. 203–214.

Bella, P., Haviarová, D., Kováč, Ľ., et al., 2014. Jaskyne Demänovskej doliny [Caves of the Demänovská Valley]. ŠOP SR, SSJ, Liptovsky Mikuláš: 200.

Borsato, A., Frisia, S., Fairchild, I.J., et al., 2007. Trace element distribution in annual stalagmite laminae mapped by micrometer-resolution X-ray fluorescence: implications for incorporation of environmentally significant species. Geochim. Cosmochim. Acta 71, 1494–1512.

Droppa, A., 1957. Demänovské Jaskyne, Krasové Zjavy Demänovskej Doliny [Demänovské Caves, Karst Landforms of the Demänovská Valley]. SAV, Bratislava. pp. 289.

Droppa, A., 1966a. The correlation of some horizontal caves with river terraces. Stud. Speleol. 1, 186–192.

Droppa, A., 1966b. Typisation of the karst region in the carpathians. Problems Speleol. Res. 2, 23–32.

Droppa, A., 1972. Geomorfologické pomery demänovskej doliny [geomorphology of Demänová valley]. Slov. Kras. 10, 9–46.

Fairchild, I.J., Baker, A., 2012. Speleothem Science: from Process to Past Environments. John Wiley & Sons.

Fairchild, I.J., Hartland, A., 2010. Trace element variations in stalagmites: controls by climate and by karst system processes. Ion Partitioning Ambient-Temperature Aqueous Syst. 10, 259–287.

Fairchild, I.J., Smith, C.L., Baker, A., et al., 2006. Modification and preservation of environmental signals in speleothems. Earth-Science Rev. 75, 105–153.

Fohlmeister, J., Schröder-Ritzrau, A., Scholz, D., et al., 2012. Bunker Cave stalagmites: an archive for central European Holocene climate variability. Clim. Past 8, 1751–1764.

Fohlmeister, J., Vollweiler, N., Spötl, C., et al., 2013. COMNISPA II: update of a mid-European isotope climate record, 11 ka to present. Holocene 23, 749–754.

Herich, P., 2015. 40 km v Demänovskom jaskynnom systéme [40 km in Demänová cave system]. Sprav. Slov. Speleol. spoločnosti 46, 11–13.

Hoffmann, D.L., 2008. Th-230 isotope measurements of femtogram quantities for U-series dating using multi ion counting (MIC) MC-ICPMS. Int. J. Mass Spectrom. 275, 75–79.

Hoffmann, D.L., Pike, A.W., García-Diez, M., et al., 2016. Methods for U-series dating of CaCO 3 crusts associated with Palaeolithic cave art and application to Iberian sites. Quat. Geochronol. 36, 104–119.

Hoffmann, D.L., Prytulak, J., Richards, D.A., et al., 2007. Procedures for accurate U and Th isotope measurements by high precision MC-ICPMS. Int. J. Mass Spectrom. 264, 97–109.

Holko, L., Dóša, M., Michalko, J., et al., 2012. Isotopes of oxygen-18 and deuterium in precipitation in Slovakia [Izotopy kyslíka-18 A deutéria v zrážkach na Slovensku]. J. Hydrol. Hydromechanics 60, 265–276.

IAEA/WMO, 2017. Global network of isotopes in precipitation. The GNIP database. Accessible at: http://www.iaea.org/water.

Kelly, M.J., Edwards, R.L., Cheng, H., et al., 2006. High resolution characterization of the Asian Monsoon between 146,000 and 99,000 years BP from Dongge Cave, China and global correlation of events surrounding Termination II. Palaeogeogr. Palaeoclimatol. Palaeoecol. 236, 20–38.

Latham, A., Schwarcz, H., 1992. Carbonate and Sulphate Precipitates. Uranium-series Disequilibrium: Applications to Earth, Marine, and Environmental Sciences, 2. ed.

Liu, W., Martinón-Torres, M., Cai, Y-j, et al., 2015. The earliest unequivocally modern humans in southern China. Nature 526, 696–699.

McCann, T., 2008. The Geology of Central Europe. Volume 2: Mesozoic and Cenozoic. The Geology of Central Europe. Volume 2: Mesozoic and Cenozoic. vol. 2. The Geological Society of London, pp. 1449.

McDermott, F., Atkinson, T., Fairchild, I.J., et al., 2011. A first evaluation of the spatial gradients in δ 18 O recorded by European Holocene speleothems. Glob. Planet. Change 79, 275–287.

Motyka, J., Gradziński, M., Bella, P., et al., 2005. Chemistry of waters from selected caves in Slovakia—a reconnaissance study. Environ. Geol. 48, 682–692.

Osmond, J., Cowart, J., 1992. Ground water. In: Ivanovich, M., Harmon, R.S. (Eds.), Uranium-series Disequilibrium: Application to Earth, Marine, and Environmental Sciences 2nd Edt. Clarendon Press, Oxford, pp. 290–333.

Osmond, J., Ivanovich, M., 1992. Uranium-series Mobilization and Surface Hydrology. Uranium-series Disequilibrium: Applications to Earth, Marine, and Environmental Sciences, 2. ed.

Scholz, D., Hoffmann, D.L., 2011. StalAge–an algorithm designed for construction of speleothem age models. Quat. Geochronol. 6, 369–382.

Scholz, D., Hoffmann, D.L., Hellstrom, J., et al., 2012. A comparison of different methods for speleothem age modelling. Quat. Geochronol. 14, 94–104.

Spötl, C., Mangini, A., Richards, D.A., 2006. Chronology and paleoenvironment of marine isotope stage 3 from two high-elevation speleothems, Austrian Alps. Quat. Sci. Rev. 25, 1127–1136.

Wang, Y.-J., Cheng, H., Edwards, R.L., et al., 2001. A high-resolution absolute-dated late Pleistocene monsoon record from Hulu Cave, China. Science 294, 2345–2348.

Yuan, D., Cheng, H., Edwards, R.L., et al., 2004. Timing, duration, and transitions of the last interglacial Asian monsoon. Science 304, 575–578.